OCTOBER 2019
VOLUME 52
NUMBER 10
pubs.acs.org/accounts

ACCOUNTS of chemical research

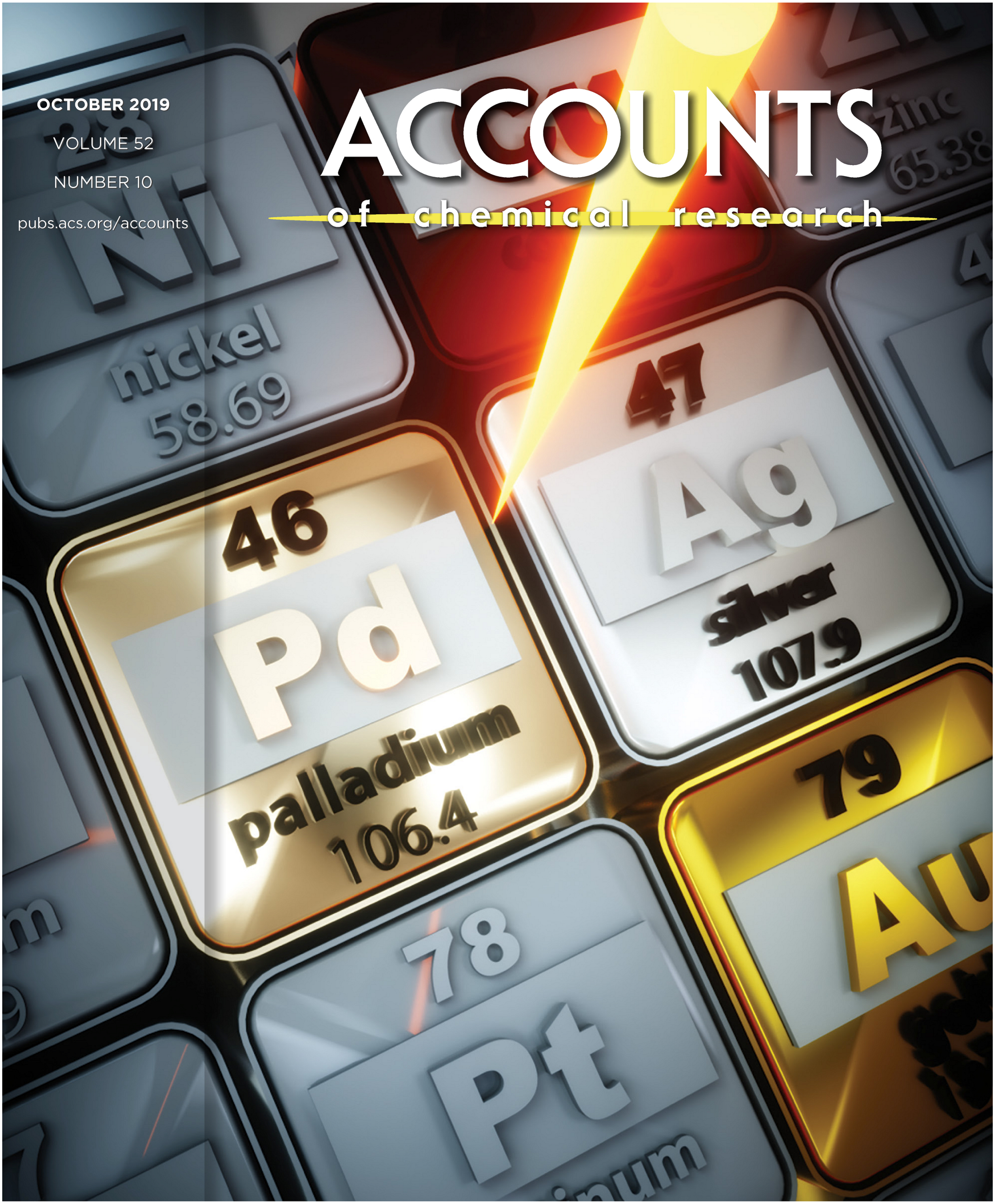

ACS Publications
Most Trusted. Most Cited. Most Read.
www.acs.org

ACCOUNTS
of chemical research

Article

Cite This: *Acc. Chem. Res.* 2019, 52, 2881−2891

pubs.acs.org/accounts

Alloying: A Platform for Metallic Materials with On-Demand Optical Response

Mariama Rebello Sousa Dias[†] and Marina S. Leite*[,‡,§]

[†]Department of Physics, University of Richmond, Richmond, Virginia 23221, United States
[‡]Department of Materials Science and Engineering, University of Maryland, College Park, Maryland 20742, United States
[§]Institute for Research in Electronics and Applied Physics, University of Maryland, College Park, Maryland 20742, United States

CONSPECTUS: Metallic materials with engineered optical properties have the potential to enhance the performance of energy harvesting and storage devices operating at the macro- and nanoscale, such as solar cells, photocatalysts, water splitting, and hydrogen storage systems. For both thin films and subwavelength nanostructures, upon illumination, the coherent oscillation of charge carriers at the interface with a dielectric material gives rise to resonances named surface plasmon polariton (SPP) and localized surface plasmon resonance (LSPR), respectively. These resonances result in unique light absorption, scattering, and transmission responses over the electromagnetic spectrum, which, in turn, can be exploited to tailor the behavior of active metallic components in optoelectronic devices containing Ag, Au, Cu, Al, Mg, among other metals. The wavelength in which the resonances occur primarily depends on the metal itself (i.e., the dielectric function or permittivity), the dielectric medium surrounding the metals, and the size, geometry, and periodicity of the metallic nanostructures. Nevertheless, the aforementioned parameters allow a limited modulation of both SPP and LSPR over a narrow window of frequencies. To overcome this constraint, we have proposed and realized the alloying of metals via physical deposition methods as a paradigm to almost arbitrarily tuning their optical behavior in the UV-NIR, which leads to permittivity values currently not available. Our approach offers an additional knob, chemical composition, to engineer light-matter interactions in metallic materials.

This Account highlights recent progress in using alloying as a pathway to control the optical behavior of metallic thin films and nanostructures for energy harvesting and storage applications, including (photo)catalysis, photovoltaics, superabsorbers, hydrogen storage, among other systems. We choose to primarily focus on the optical properties of the metallic mixtures and in their near- to far-field responses in the UV-NIR range of the spectrum as they represent key parameters for materials' selection for the devices above. By alloying, it is possible to obtain metallic materials with LSPR not available for pure metals, which can enable the further control of the electromagnetic spectrum. First, we discuss how the permittivity of binary mixtures of coinage metals (Au, Ag, and Cu) can be tailored based on the chemical composition of their pure counterparts. Second, we present how novel metallic materials can be designed through band structure engineering through density functional theory (DFT), a paradigm that could benefit from artificial intelligence methods. Concerning alloyed thin films, we discuss the promise of earth-abundant metals and provide an example of the superior performance of AlCu in superabsorbers. In the realm of nanostructures, we focus the discussion on physical deposition methods, where we provide a detailed analysis of how chemical composition can affect the far- and near-field responses of metallic building blocks. Finally, we provide a brief outlook of promising next steps in the field.

1. INTRODUCTION

Plasmonics is the field of study that explores the interactions between the electric field component of light and free electrons in metallic thin films and nanostructures. The oscillation of the free electrons around its positive fixed ions, termed plasmons, has a plasma frequency defined by ω_p. Light also has a characteristic frequency, and when interacting with metals, one observes either reflection (incident light with a frequency below ω_p) or transmission (incident light with a frequency above ω_p). At the interface of metals and dielectrics, the plasmons interacting with light result in a surface plasmon polariton (SPP) excitation: a strongly confined surface wave that propagates along the interface. In nanoscale structures with dimensions smaller than the wavelength of light, localized surface plasmons are produced, as a result of the confinement of an SPP. At the plasmon resonant frequency, or localized surface plasmon resonance (LSPR), light is mostly absorbed by the nanostructures, leading to an enhanced electric field at its vicinity. This unique confinement effect has been applied to improve the performance of a variety of energy harvesting and storage processes, ranging from (photo)catalysis,[1] photovoltaics,[2] superabsorbers,[3] to hydrogen storage.[4] A very effective knob for tuning the optical response of the metallic thin films and nanostructures to finely tailor the wavelength range for SPP and LSPR is to modify their chemical

Received: March 25, 2019
Published: July 15, 2019

DOI: 10.1021/acs.accounts.9b00153
Acc. Chem. Res. 2019, 52, 2881−2891

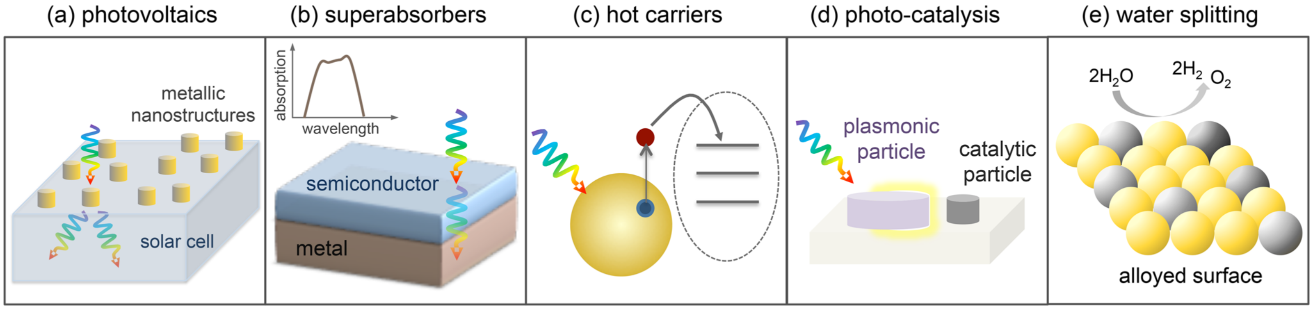

Figure 1. Examples of energy generation systems based on metals that can benefit from the development of metallic alloys and mixtures. Out of scale for clarity.

composition by alloying,[3,5−9] as will be discussed in this Account. Moreover, the control of the electromagnetic spectrum has also enabled the further development of a variety of optoelectronic devices, such as switches,[10] biosensors,[11] and displays.[12]

Concerning the suitability of metallic materials for controlling LSPR and SPP, noble metals such as Ag, Au, Pt, and Pd have been a primary choice due to their abundant free electrons despite well-known optical losses due to interband optical transitions.[13] In the last years, earth-abundant metals (Al and Mg) have presented themselves as a burgeoning new class of materials for low-optical-loss and low-cost optical components.[14] Although countless examples of photonic devices have been reported in the literature, the wavelength of the resonance excitations is restricted to a specific range of the electromagnetic spectrum mainly due to the fixed and well-defined dielectric function (permittivity, $\varepsilon = \varepsilon_1 + i\varepsilon_2$) of the metals. Thus, their applications toward renewable energy are still somewhat restricted. One alternative to overcome this limitation is to modify the dimensions and geometry of the metallic nanoscale building blocks, which has allowed some tunability of their optical behavior.[15−17] Bimetallic and multicomponent mixtures can provide an almost on-demand modulation of the materials' optical response (e.g., engineered values of ε_1 and ε_2), spanning beyond the ultraviolet (UV) and the near-infrared (NIR).[5,18−20] While colloidal synthesis has been the pioneering route for obtaining alloyed photonic nanostructures,[21,22] this Account focuses on fabrication methods based on physical deposition, which enables high control of the building blocks orientation and arrangement within a substrate.

2. THE NEED FOR METAL ALLOYS IN ENERGY HARVESTING AND STORAGE

Metallic alloys represent a promising platform for enhancing the performance of energy harvesting and storage systems. Concerning energy generation, metallic thin films and nanostructures have proven to be very useful as an active component in photovoltaics (PV)[23] and hot carrier devices,[24] among others. In the realm of energy storage, there are countless examples of hydrogen storage systems using metals.[4] Figure 1 displays some of the significant examples of how metals can be incorporated into energy-related devices. In particular, metallic nanostructures have been successfully implemented for concentrating and trapping light in PV devices because of the excitation of surface plasmons. They can increase light absorption in the semiconductor material by essentially three mechanisms: by reducing reflection through increased forward scattering; by increasing the local fields throughout the excitation of localized plasmon resonances, acting as "antennas"; and by incident light coupling into waveguide modes of the solar cell material (waveguiding), which significantly increases the optical path length within the semiconductor.[25] Depending on device architecture and on what type of solar cell material, the nanostructures can be added to the top, the middle, or the bottom (light back reflector) of the solar cell stack (see Figure 1a). Both Ag and Al have been seen to effectively improve the performance of Si and III−V solar cells,[26] while Au seems to work best for organic photovoltaics. In all cases, it would be ideal if one could tune the resonance wavelength of the nanostructures to finely adjust it to the solar spectrum, which can be achieved by mixing metals. As shown in Figure 1b−d, in systems where it is desired that the metal absorbs light, there is a need for large ε_2, such as in hot carrier devices[24,27] and superabsorbers.[3] In the former, the plasmon excitations in the metals are used to produce charge carriers with energy larger than the equivalent thermal excitation at ambient temperature. This phenomenon has been successfully implemented in a variety of situations, including in the photodissociation of H_2 and O_2 molecules[24] and to lower the energy barrier of catalytic processes.[28] Here, the efficiency of the energy conversion processes involved is highly dependent on the Fermi level of the metal and, indirectly, ε. The latter consists of devices that present near unity absorption; all incident radiation is absorbed independently of the frequency (transmission, reflection, and scattering events are negligible).

The basis of traditional catalysis relies on metals dispersed onto high surface area support materials, and involves high-temperature reactions. Nevertheless, light-driven chemical reactions are preferred, where LSPR in the metallic nanostructures leads to phonon-driven or charge-carrier-driven mechanisms that result in lower activation energies.[29] A current major challenge in photocatalysis is related to the limited number of active and low-cost metals. While several transition metals are considered good catalysts (Pd, Pt, Ru, etc.), they are often seen as restricted plasmonic materials because of their modest light absorption within the visible range of the spectrum. Thus, the possibility of combining the advantages of catalytic metals with plasmonic properties is a potential solution for achieving high performing catalysts involving room temperature activation mechanisms. Figure 1d depicts an example of a so-called "antenna-reactor" system,[30] where a catalytic metal and a plasmonic one are combined to promote light-driven reactions. Note that we have recently demonstrated that Pd−Au alloyed thin films outperform pure Pd in catalytic reactions of ethanol oxidation in alkaline media,[9] and we anticipate these alloys to be implemented in

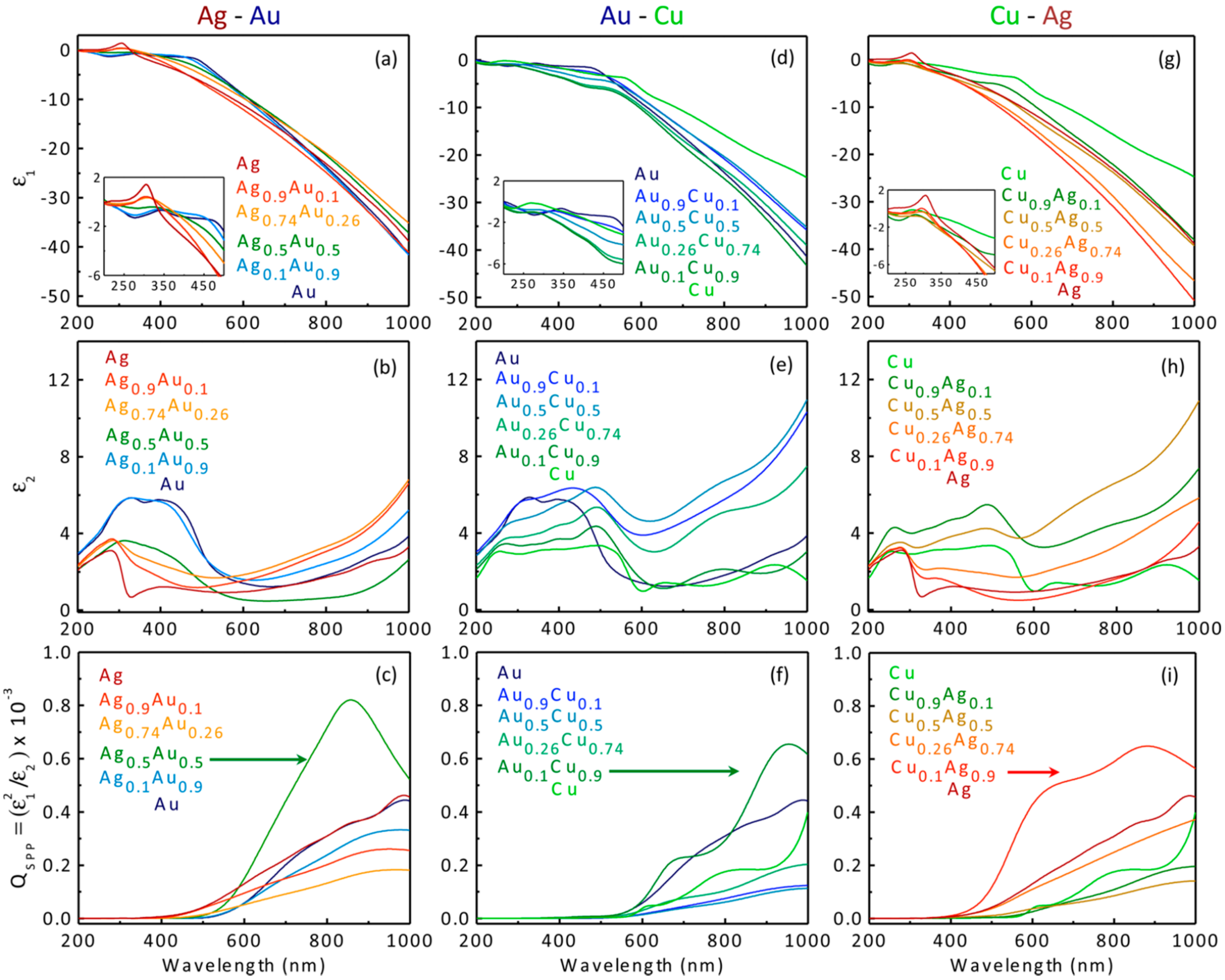

Figure 2. Real (ε_1) and imaginary (ε_2) parts of the dielectric function of alloyed thin films determined by ellipsometry, and quality factor for all mixtures. Reproduced with permission from ref 5. Copyright 2019 American Chemical Society.

the "antenna-reactor" configuration as described in Figure 1d in the near future.

Despite the multiple successful demonstrations of metals as active components of energy harvesting and storage systems, there is a consensus that the final performance of the devices can strongly depend on their optical properties, as expected. Hence, finding metallic materials that can boost these devices' performance is of primary interest to chemists, physicists, and engineers working in research and innovation related to renewable energy. The ability to further control the electromagnetic spectrum, i.e., light absorption, transmission, and reflection, will enable the realization of energy-related devices with superior performance. A practical solution is to mix metals, as we have demonstrated. This first step toward overcoming the limitation of the predetermined permittivity of metals is discussed in detail in this Account.

3. OPTICAL BEHAVIOR OF BINARY METALLIC MIXTURES

A primary challenge for the further development of photonic components for energy harvesting and storage that operates in the UV-NIR range of the spectrum is related to the predefined permittivity of metals, as stated earlier. This constrains light absorption, transmission, and reflection, which, in turn, limits light interactions with the metal. To address this drawback, we recently proposed and demonstrated how the alloying of metals could provide values of permittivity not found in the pure metals available in the periodic table within the UV-NIR.[5] Because the precise design of metallic components with controlled optical response relies on ε, we first developed a library for the binary metallic mixtures of coinage metals, as shown in Figure 2. Briefly, all thin film samples are fabricated by cosputtering deposition, which produces thin films with controlled chemical compositions and thicknesses. For determining ε, we acquired spectroscopic ellipsometry measurements.

Spectroscopic ellipsometry is an ideal method to determine the permittivity of metallic thin films. Here, broadband light is reflected or transmitted by the thin films deposited on a transparent substrate. Commonly, three incident angles (60, 65, and 75°) are used for the reflection and a normal incident angle (0°) for the transmission measurement. The ellipsometry data is then modeled by B-spline functions to determine ε of the mixtures, where we always ensure the Kramers−Kronig relation. Figure 2 shows both the real (ε_1) and imaginary (ε_2)

parts of ε and the quality factor of the SPP for bimetallic thin films formed by Ag, Au, and Cu. These materials have been extensively implemented in optical devices operating in the UV-NIR. The Ag−Au mixture (Figure 2a−c) forms a solid solution over the entire range of compositions. Thus, an almost monotonic red-shift of the interband transition from pure Ag (300 nm) to pure Au (500 nm) is verified, which is characterized by the sudden change in ε_2. For the Au−Cu system (Figure 2d−f), we also observed a linear shift from Au (500 nm) to Cu (550 nm). However, for the Cu−Ag films (Figure 2g−i), there is no linear transition, and both peaks from Cu (530 nm) and Ag (300 nm) are concomitantly observed for the entire range of compositions. This result indicates that both Ag and Cu are contributing independently, and no solid solution is formed in this case, as expected from the phase diagram of this system.[31] Note that Ag−Cu alloys can be achieved by postdeposition quenching or UV light-treatment in a nitrogen atmosphere.[32−34] Figure 2c, f, and i demonstrates how a bimetallic material can outperform its pure counterparts in terms of its SPP quality factor, defined as $Q_{SPP} = (\varepsilon_1^2/\varepsilon_2)$.[24] We found that $Ag_{0.5}Au_{0.5}$, $Au_{0.1}$, $Cu_{0.9}$, and $Cu_{0.1}Ag_{0.9}$ have a higher Q_{SPP} then their respective pure elements for a certain part of the electromagnetic spectrum, a situation where the mixtures are "more than the sum of its parts". Generally, low values of ε_2 translate into high Q_{SPP}. As somewhat expected, the experimental parameters used during thin film deposition can substantially affect grains size and defect density. These variations often lead to distinct permittivity values, as reported in the literature.[35] Here, the origin of the unique behavior for Ag−Au can be explained in terms of the highly disordered $Ag_{0.5}Au_{0.5}$ alloy.[5,36] In Au−Cu mixtures, the effect of order/disorder can be easily veiled by the scatter band resulting from variations in thin film deposition parameters.[37] Finally, Ag−Cu is known for requiring a postdeposition quenching step to enable alloying (not performed here). As a result, the spectra for this metal combination present two well-defined absorption edges at 300 and 530 nm, indicating the independent contribution from both metals. Overall, these alloyed thin films can be easily scaled up, critical for their commercialization.

4. DESIGN OF METALLIC MATERIALS THROUGH BAND STRUCTURE ENGINEERING

The interplay between the optical and electronic properties of the alloys is particularly relevant for photocatalysis, water-splitting systems, and surface-enhanced Raman scattering.[28,38] Therefore, establishing a direct correction between the optical and electronic response of the metal alloys is key for designing metallic materials with tailored optical behavior. By determining their band structure, one can resolve how their interband transitions relate to optical absorptions. X-ray photoelectron spectroscopy (XPS) is an accurate experimental method for resolving the valence band spectra of metallic materials, ideal for probing thin films. We measured XPS on Ag−Au alloyed films and built a detailed connection with its optical transmission. As presented in Figure 3a and b, the separation between the $d_{3/2}$ and $d_{5/2}$ bands increases nonlinearly (Figure 3b) as the Au content rises,[7] which all correspond to electronic transitions in the visible range of the electromagnetic spectrum. Moreover, the increase in the Au concentration leads to a $d_{5/2}$ broadening;[7] constituting the minimum onset binding energy required for optical excitation. In turn, this change in the d band causes both the optical transmission peak and the SPP to broaden; see Figure 3c. Quantitatively, the onset of $d_{5/2}$ and the transmission peak for $Ag_{0.50}Au_{0.50}$ occur at 2.05 and 2.40 eV, respectively, suggesting that the tunability for the interband transition is possible due to the energy shift of the d band within the material. Our density functional theory (DFT) calculations confirmed this result, as will be discussed in the next paragraph.

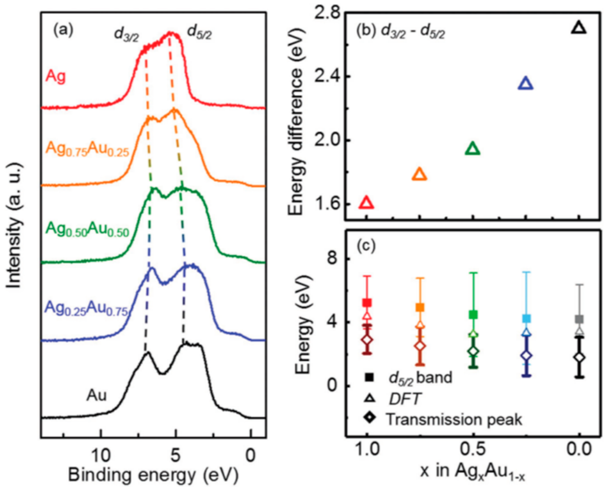

Figure 3. (a) XPS measurements of the valence band of Ag−Au alloyed thin films. (b) Energy difference between the two d band peaks. (c) Energy of the $d_{5/2}$ band peak, maximum of the transmission spectra, and band transition calculated by DFT. Reproduced with permission from ref 7. Copyright 2018 WILEY-VCH Verlag GmbH & Co.

The most accurate method to determine the complete band structure of metals is DFT, where the number of atoms required to represent the unit cell of a mixture depends on the symmetry of the pure constituents, the enthalpy for alloying, and the material's final chemical composition. The majority of simulations probing metal alloys for photonics have focused on describing their electric field profiles and decay (primarily through finite-difference time-domain, FDTD). While very informative, these methods do not convey the correlation between the optical and electronic properties of materials, which is a crucial factor when designing devices. Driven by the necessity to fully depict the metal alloys characteristics, we have implemented DFT to predict the correlation between their electronic and optical response.[7] Figures 4 and 5 show the band structures of Ag_xAu_{1-x} and Pd_xAu_{1-x} alloys. The color palettes depict the weight contribution of each pure metal to the overall band structure, as the hues represent their weight on each wavevector-dependent electronic state. This information is critical to resolving which element dominates the interband transitions measured by spectroscopic ellipsometry. For Ag and Au (Figure 4), the optical transitions occur in the isotropic and symmetric Γ and R points, with the former corresponding to the unit cell's critical point. As the Au content increases, the d band moves closer to the Fermi level at the Γ point. This results in a reduction of the energy gap between the first empty state and the d band. This modification of the band structure with chemical composition points out to a shift of the interband transition to a longer wavelength. Here, our valence band calculations obtained by DFT can be compared with the experimental values acquired from XPS. There is a good agreement between the change in the energy for the interband transition (quantified by DFT),

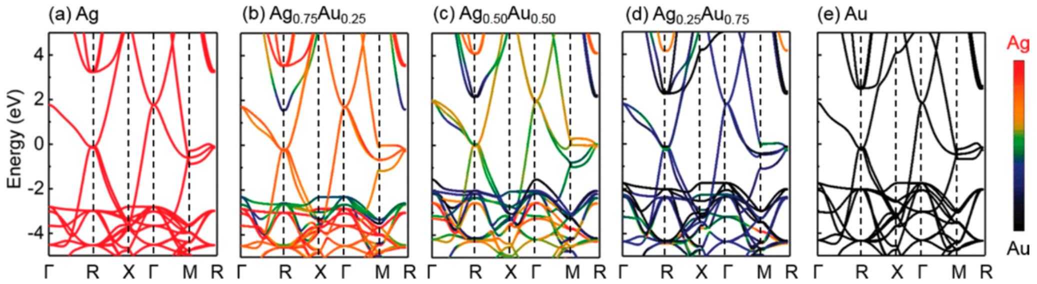

Figure 4. Band structure of Ag_xAu_{1-x} alloys calculated by density functional theory. Note that the color of the bands (ranging from red to black) refers to the individual contributions of Ag and Au, respectively. Reproduced with permission from ref 7. Copyright 2018 WILEY-VCH Verlag GmbH & Co.

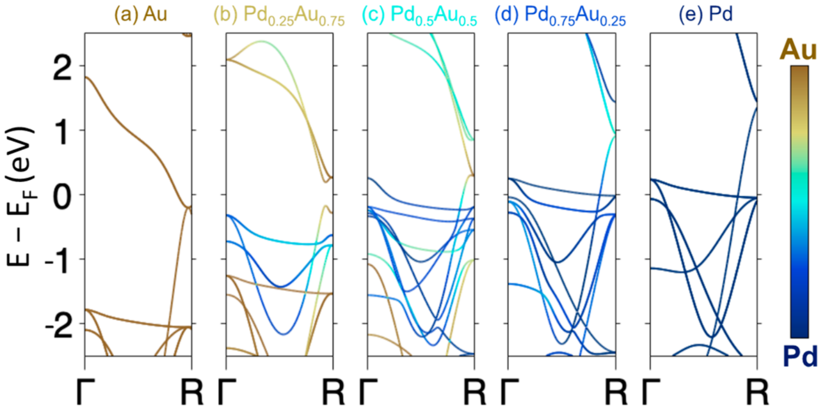

Figure 5. Band structure of Pd_xAu_{1-x} alloys calculated by density functional theory. The color palette indicates the contribution of the Pd (navy) and Au (dijon) to the electronic bands. Reproduced with permission from ref 9. Copyright 2019 American Chemical Society.

the valence band spectra (VBS), and the optical transmission measurements (see Figure 3c). We note that while both Ag and Au present comparable contributions to most states of Γ point, Au dominates the majority of the *d* band states with energy ranging between −2.0 and −3.0 eV, as shown in Figure 4c for $Ag_{0.5}Au_{0.5}$, a consequence of the ≈1.6 eV higher energy of the *d* band of Au.

As an additional example of how DFT can be employed to unravel the electronic characteristic of the metal alloys, we also present the band structure of a series of Pd−Au alloys, an effective catalyst in oxidation processes in ethanol, formic acid, benzyl alcohol, among others.[9] The FCC symmetry of both Pd and Au leads to highly degenerated bands even for the mixtures; see Figure 5. For this metal combination, the Pd atoms dominate the profiles and values of the new *d* bands near the Fermi level E_F (from −2.0 eV to +0.3 eV) that emerge from alloying at the Γ point. There is a strong hybridization close to E_F for $x \geq 0.25$. The nonlinear decrease in the energy gap between the *d*-band and the first empty state (>1.0 eV) indicates that the interband transitions in Pd_xAu_{1-x} can be engineered upon a refined chemical composition control, where one can predict the wavelength of maximum light absorption and use this property to accelerate photocatalytic reactions[9] and hydrogen storage.[39] These results highlight the importance of analyzing each metal combination individually, where distinct behaviors are often revealed by DFT. Overall, the information provided by DFT is extremely insightful, as it can describe all relevant electronic bands (and possible electronic transitions).

5. ALLOYED THIN FILMS FROM EARTH-ABUNDANT METALS FOR PHOTONICS

For on-chip nanophotonics, metals like Al and Cu are ideal due to their fully complementary metal−oxide−semiconductor (CMOS) compatibility and earth abundance, resulting in low-cost device processing. Similar to the aforementioned noble metals, these materials have well-defined ε, which equally limits their application. Thus, we have extended our alloying paradigm to assess how a mixture between Al and Cu thin films can enable superabsorber devices with superior performance. Our detailed and systematic comparison between AlCu and the most commonly used metals is presented in Figure 6.[3] The top row of the Figure depicts the configuration of the bilayer structure responsible for light superabsorption, which consists of a thin film Si layer with variable thickness and a metallic back reflector with 100 nm. Figure 6a−l shows how the thickness of the Si top layer modulates the resonant absorption peak from the UV to the NIR. The addition of an AlCu alloyed thin film is particularly interesting for attaining near-unity light absorption (>99%), an effect that cannot be achieved by pure metals in a thin film configuration. Further, we can tune the wavelength of this ultrahigh absorption over a broad portion of the electromagnetic spectrum (from λ = 409 nm to λ = 1016 nm) by simply modifying the thickness of the semiconductor layer. Figure 6m−r highlights the omnidirectional property of our planar configuration: the angle of the incident light does not affect the absorption of it for oblique angles of incidence (<70%).

The search for metallic building blocks for photonics that are CMOS-compatible and earth-abundant triggered intense research with Al in the last five years. Since then, Al films and

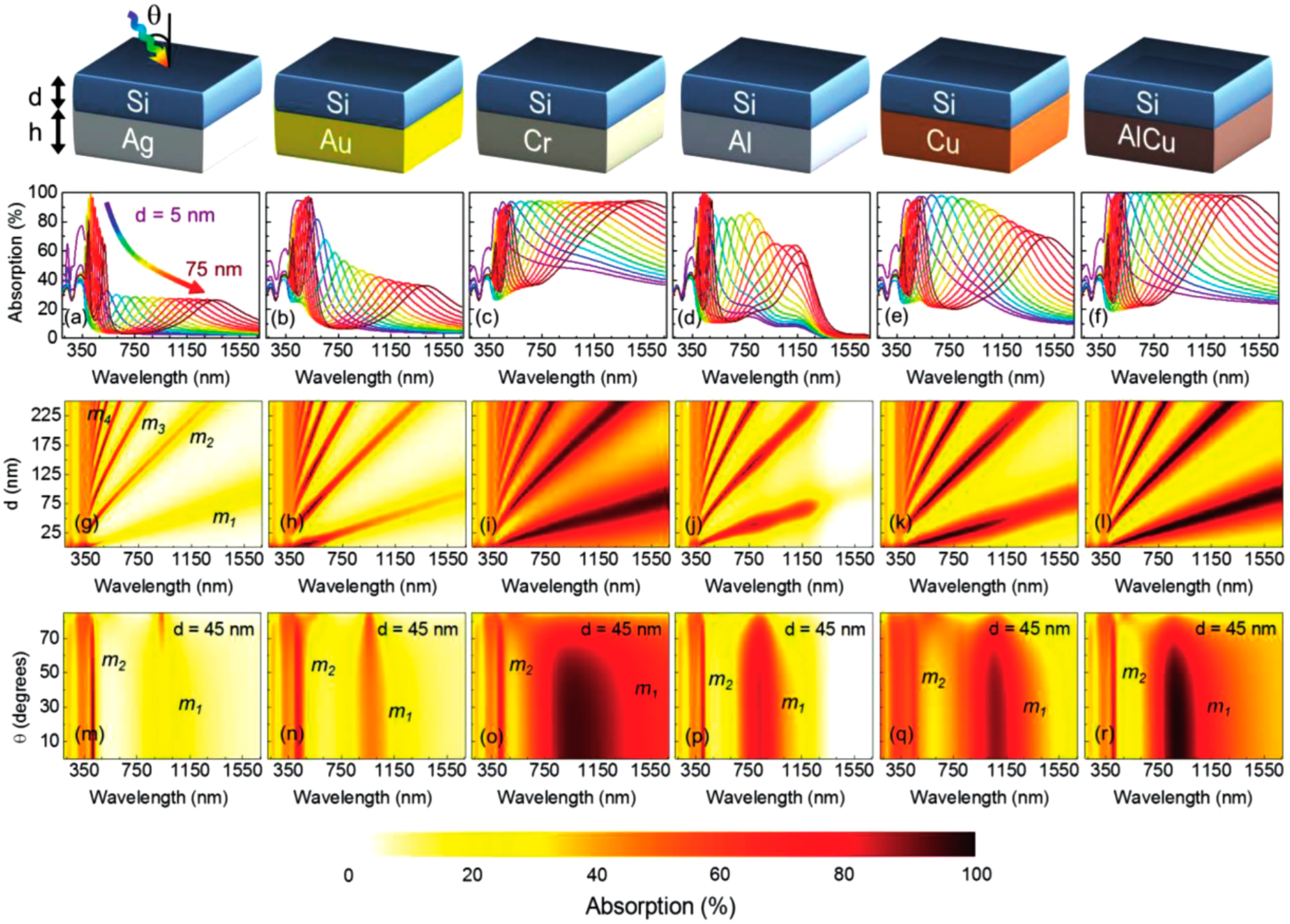

Figure 6. (Top row) Illustrations of thin film architecture for superabsorbers formed by a top Si layer (with variable thickness *d*) and a metallic back reflector (with thickness $h = 100$ nm). θ refers to light's angle of incidence. (a−f) Calculated absorption spectra for normal light incidence as a function of the thickness of the Si layer for different metallic substrates, including a AlCu mixture. (g−l) Calculated absorption maps as a function of *d* highlighting the existence of more than one absorption mode (m_i). (m−r) Calculated absorption maps as a function of the angle of the incident light for $d = 45$ nm. Reproduced with permission from ref 3. Copyright 2018 WILEY-VCH Verlag GmbH & Co.

nanoarchitectures have been successfully employed to boost the performance of energy harvesting systems such as superabsorbers,[40] photovoltaics,[41] and catalysts,[42] as well as in color pixels. Although Al is the third most abundant element on the Earth's crust, it is not biodegradable. Therefore, we have recently proposed Mg as a biodegradable, biocompatible, and low-loss metal for photonics.[43] We have implemented a novel platform for photonics based on Mg (metal) and MgO (dielectric) for biodegradable color pixels that can vanish upon the controlled exposure of these materials to water.[43] This work opened the door for the further development of transient photonic devices, ideal for hiding and revealing information in a controlled manner (e.g., encryption). Moreover, we anticipate that intricate three-dimensional structures of Mg could be obtained through the fabrication of Mg-metal structures, followed by selective etching procedures. Selective etchings are currently well developed for a wide range of materials, spanning a large variety of semiconductors and metals.[44] Almost simultaneous to our work, it has been shown that the hydrogenation/dehydrogenation of Mg nanostructures leads to dynamic color pixels.[45] There are still enormous opportunities for the development of Mg-based alloys, where their optical behavior could be tailored based on their geometry and degree of mixture.

6. ALLOYED NANOSTRUCTURES WITH TAILORED OPTICAL RESPONSE

This section of the Account focuses on how alloying is an effective pathway to tailor the LSPR in nanostructures, which is a powerful knob to further tailor permittivity. Acknowledging that, traditionally, alloyed metallic nanostructures have been primarily fabricated via chemical synthesis,[28,46,47] we emphasize here physical deposition methods because of the freedom associated with the nanoparticles' final dimensions, geometry, and chemical composition, and due to the lack of organic ligands (that can severely alter light−matter interactions). In nanophotonic systems, uniformity in surface coverage and optimization of the surface density are required; and both can be attained by physical deposition methods. Recent developments in physical deposition techniques of alloyed metal subwavelength structures, from self-organization to nanolithography, have permitted their use as building blocks for electrocatalysis,[48] electrochemical energy applications,[49] and hydrogen sensors.[50] Scanning probe lithography methods can precisely control the chemical composition of generating bimetallic nanoparticles, although the overall diameter of the particle stays in the 2−50 nm range.[51] Alternatively, templates have been used to fabricate arrays of alloyed nanoparticles

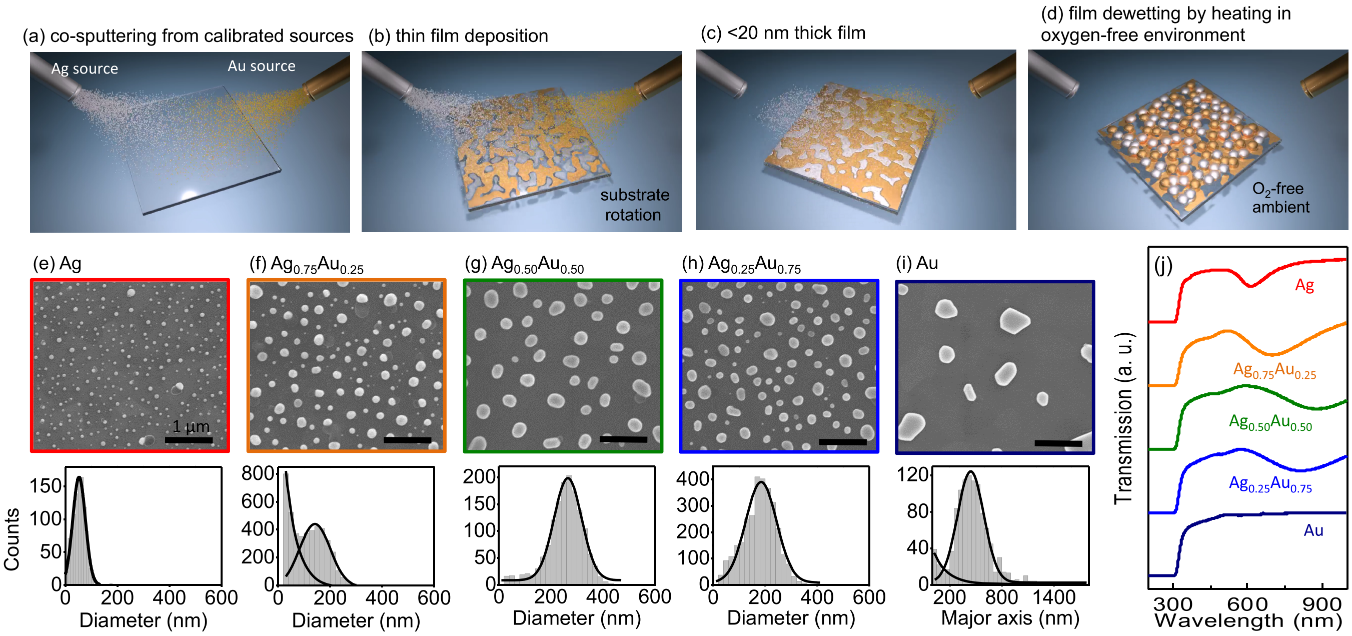

Figure 7. (a–d) Illustration of step-by-step scalable cosputtering deposition process for obtaining alloyed nanoparticles. Adapted with permission from ref 8. Copyright 2019 Elsevier Ltd. (e–i) SEM images of Ag$_x$Au$_{1-x}$ formed by cosputtering. The bottom row shows the respective diameter statistics. (j) Optical transmission measurements for nanoparticles shown in (e)–(i). Reproduced with permission from ref 6. Copyright 2017 WILEY-VCH Verlag GmbH & Co.

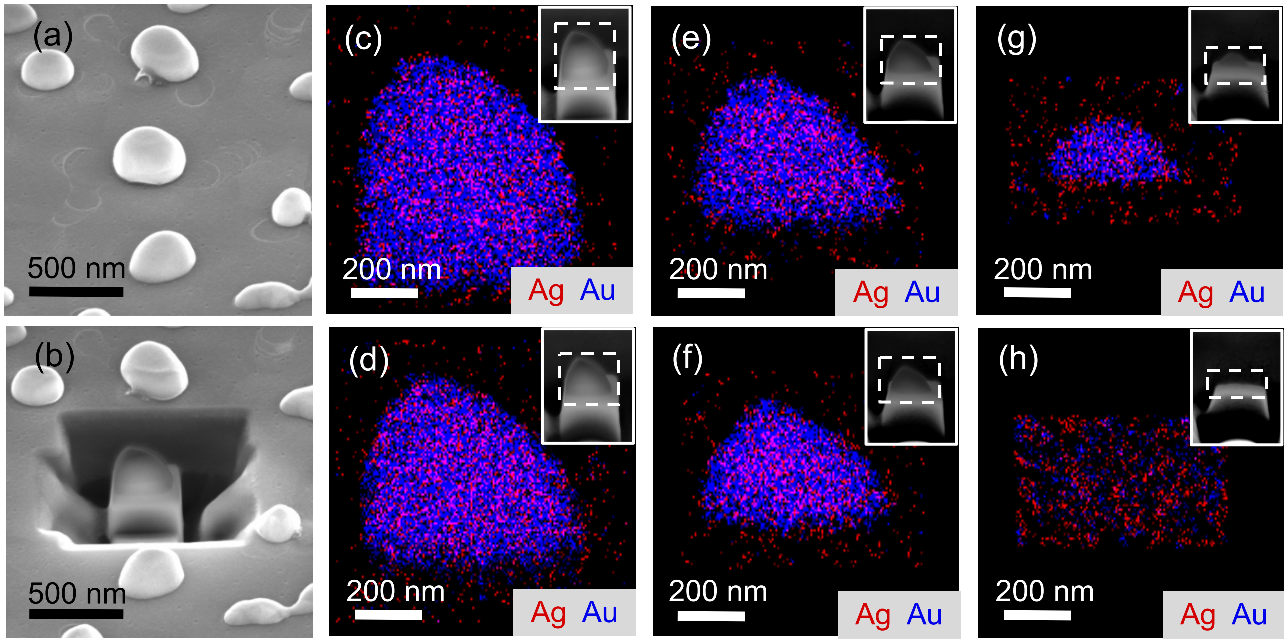

Figure 8. (a, b) SEM images of Ag–Au nanostructures fabricated by the dewetting process of thin films. (c–h) Sequence of EDS images showing a uniform distribution of both Ag and Au in a representative nanoparticle. Reproduced with permission from ref 6. Copyright 2017 WILEY-VCH Verlag GmbH & Co.

where thin films of the alloy elements are evaporated on a nanohole mask following thermal annealing treatments to form the alloys.[52] Sequential pulsed laser deposition is another method for producing alloyed nanostructures.[53]

Concerning fabrication methods, a scalable and reliable route for metal nanostructures consists of the dewetting of ultrathin films.[6] As presented in Figure 7a–d, the first step consists in depositing the metallic elements on a substrate through cosputtering. While an ultrathin film is formed, the substrate is constantly rotated, to ensure a uniform chemical composition distribution. Note that a controlled gradient in composition and, therefore, nanoparticles' size can be obtained by not rotating the substrate. Second, the film is annealed in an O$_2$-free atmosphere to prevent oxidation. During the annealing process, dewetting of the film occurs due to surface diffusion, which results in the formation of three-dimensional nanoscale structures that minimizes the system's energy. The final size, shape, and spatial distribution (density) of the particles are determined by the thickness of the film, the type of substrate used, the annealing conditions (including temperature and

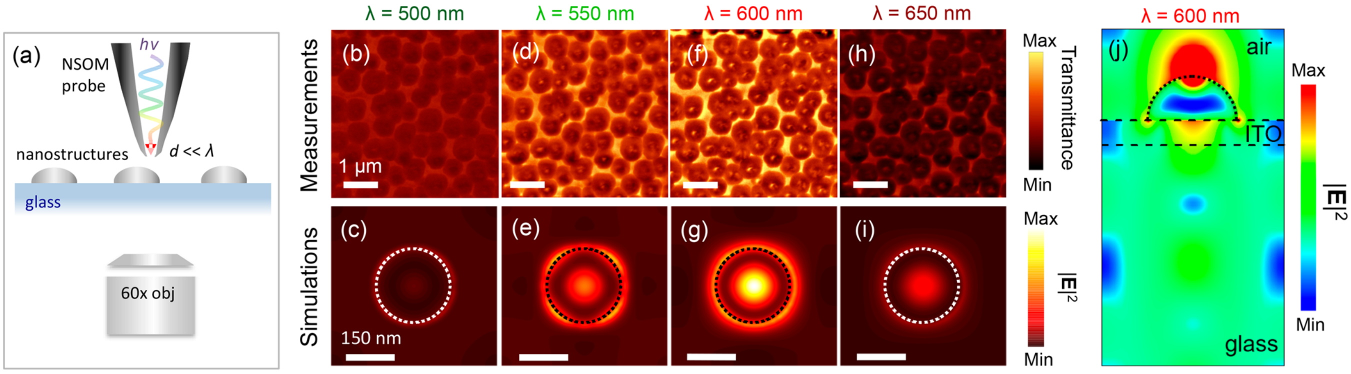

Figure 9. (a) Cross-section illustration of spectrally dependent near-field scanning microscopy (NSOM) measurement for $Ag_{0.5}Au_{0.5}$ in transmission mode. (b–i) NSOM measurements and FDTD simulations as a function of the wavelength of the incident light for $Ag_{0.5}Au_{0.5}$. (j) Simulation of electric field profile upon 600 nm excitation. Adapted and reproduced with permission from ref 6. Copyright 2017 WILEY-VCH Verlag GmbH & Co.

time), and the ratio between cohesion and adhesion among the materials. This self-assembly method allows us to obtain arrays of fully alloyed nanoparticles. As shown in Figure 7e–i for Ag–Au, nanoparticle size can be controlled by varying their composition, despite the same film thickness (10 nm).[6] These nanostructures have well-defined transmission signatures, with the wavelength of the transmission maximum primarily determined by their permittivity (see Figure 7j). In this particular case, the nanoparticles were distant enough from each other, and there was no coupling between them. Coupling is relevant because it influences the magnitude of the electric fields,[54] so-called "hot spots", and can be achieved by tuning the post-thin film deposition annealing conditions. Alternatively, template deposition followed by annealing is another route for controlling the spacing between the nanostructures, as well as their shape, which can narrow the LSPR down to 1–2 nm in spectral width.[55] Moreover, when particles are nearby, spectral shifts of the plasmonic resonances and modification and splitting of their line-shapes can occur.[56]

In order to confirm the alloying of metals down to the nano- and atomic scales, the scientific community has utilized traditional and advanced chemical composition characterization methods, including energy dispersive X-ray spectroscopy (EDS) using both scanning and transmission electron microscopy (SEM and TEM), electron energy-loss spectroscopy (EELS), and high-angle annular dark-field imaging (HAADF).[6,52,57,58] The relevance of determining the distribution of each metal constituent lies in identifying how alloying takes place at the nanoscale, and how material segregation can be suppressed. As an example, Figure 8 displays a sequence of EDS maps on a representative $Ag_{0.5}Au_{0.5}$ nanoparticle. Here, the nanostructured is sequentially milled using a Ga+ focused ion beam (FIB) and imaged. We determined the elemental uniform distribution within the nanoparticle, which confirms that no material segregation took place during the post-deposition annealing step. Likewise, the contrast in the HAADF-STEM image is dependent on the atomic mass, where heavier elements contribute to brighter contrast, as expected. Although beyond the scope of this Account, we certainly recognize that chemical composition mapping with high spatial resolution is key for advancing the understanding of interdiffusion processes at the nanoscale, relevant for the design of both nanostructures and ultrathin films.

The ability to confine light in extremely small regions of space and to produce electric field enhancements of orders of magnitude is paving the way to the demonstration of energy harvesting devices with superior performance. Nevertheless, the complete understanding of how light is interacting with the metallic building blocks requires spatially resolving their optical behavior at relevant length scales; this information cannot be obtained by conventional spectroscopic measurements. Near-field scanning optical microscopy (NSOM) is an ideal technique because it provides insights about *where* the "hot spots" are located. This microscopy technique is extremely versatile and can be implemented in transmission (represented in Figure 9a) or scattering mode.[6] Here, we focus the discussion on NSOM in transmission mode, and how the measurements corroborate three-dimensional simulations. As an example, we share our results of wavelength (λ) dependent NSOM measurements on $Ag_{0.5}Au_{0.5}$ nanostructures, combined with finite-difference time-domain (FDTD) simulations (Figure 9b–i).[6] We found that for a 253 nm nanoparticle the maximum transmittance occurs at λ = 600 nm (corresponding to the LSPR), in very good agreement with the macroscopic measurement presented in Figure 7j. Our simulations revealed that the first peak, at λ = 550 nm, is due to an electric quadrupole resonance, and the second, at λ = 600 nm, is an electric dipole resonance, both visualized by NSOM. Through FDTD, we also elucidated the electric field profile ($|E|^2$) for the nanostructure, as presented in Figure 9j. At the LSPR, the "hot spots" are surrounding the nanoparticle. The combination of NSOM with FDTD is a powerful approach to fully picture the behavior of light upon interacting with metallic (alloyed) nanostructures. The NSOM measurements of multicomponent alloyed structures[59] have not been exploited, and will certainly help the community predicting their design for specific applications, especially for photocatalysis.

7. CONCLUSIONS AND OUTLOOK

In this Account, we have highlighted how alloyed nanostructures are a unique platform for engineering optical responses not obtained by pure metals, very relevant for the future design of sustainable energy systems, ranging from photocatalysts to photovoltaics. The examples discussed here demonstrate the promise of alloying on the further development of optical components operating in the UV-NIR, which encompass renewable energy, and extends to defense and healthcare applications.

While alloyed structures formed by conventional metals such as Ag and Au present an array of opportunities for energy harvesting, we do recognize that there is a pressing need in our society for the usage of biodegradable materials. Moreover, the high cost of noble metals does preclude its scalability in most scenarios. Therefore, we also advocate for the further development of devices using Mg, an earth-abundant and biodegradable metal. Although the vast majority of the recent research on photonics using earth-abundant materials has focused exclusively on Al, a CMOS-compatible option that is the third most abundant element on the Earth's crust, it is neither biodegradable nor biocompatible. Nonetheless, Mg presents similar optical behavior in the UV-NIR range of the electromagnetic spectrum and is a biodegradable metal. We anticipate that this burgeoning material for photonics will also be implemented as an alloy with Al in photonics. Moreover, because Mg dissolves in water and is very low cost, it is very suitable to enable scaffold structures in which another metal (inert to water) would form the final 3D geometry as a result of material segregation.

Finally, the exquisite possibility of combining five or more metallic elements to produce polyelemental nanoscale building blocks[59] with compositional diversity and a nearly unlimited range of LSPR control will unveil new materials and functionalities. Here, determining the structure−properties−performance relationship will likely require a combined high-throughput experimental and computational effort. In the near future, we foresee artificial intelligence methods playing a significant role in determining the ideal chemical composition combinations. The materials chemistry scientific community has made remarkable advances in the fabrication and characterization of metallic thin films and nanostructures. Now, it is time to accelerate the discovery of new alloys for advancing the next-generation of metallic materials with tunable optical properties.

AUTHOR INFORMATION

Corresponding Author

*E-mail: mleite@umd.edu.

ORCID

Mariama Rebello Sousa Dias: 0000-0001-9090-0018
Marina S. Leite: 0000-0003-4888-8195

Notes

The authors declare no competing financial interest.

Biographies

Mariama Rebello de Sousa Dias is Assistant Professor of Physics at the University of Richmond. She obtained her Ph.D. at the Federal University of Sao Carlos, Brazil. Her research interests focus on optical and electronic properties of metallic and semiconductor nanostructures.

Marina S. Leite is Associate Professor in the Department of Materials Science and Engineering and in the Institute for Research in Electronics and Applied Physics at the University of Maryland. Her research encompasses functional materials, including materials for energy harvesting and storage, photonics, and novel scanning probe microscopy methods to visualize dynamic processes at the nanoscale.

ACKNOWLEDGMENTS

This Account includes work supported by NSF (DMR-1609414) and by the Schlumberger Foundation Faculty for the Future Program.

REFERENCES

(1) Christopher, P.; Xin, H.; Linic, S. Visible-Light-Enhanced Catalytic Oxidation Reactions on Plasmonic Silver Nanostructures. *Nat. Chem.* **2011**, *3*, 467.

(2) Jang, Y. H.; Jang, Y. J.; Kim, S.; Quan, L. N.; Chung, K.; Kim, D. H. Plasmonic Solar Cells: From Rational Design to Mechanism Overview. *Chem. Rev.* **2016**, *116*, 14982−15034.

(3) Dias, M. R. S.; Gong, C.; Benson, Z. A.; Leite, M. S. Lithography-Free, Omnidirectional, CMOS-Compatible AlCu Alloys for Thin-Film Superabsorbers. *Adv. Opt. Mater.* **2018**, *6*, 1700830.

(4) Schneemann, A.; White, J. L.; Kang, S.; Jeong, S.; Wan, L. F.; Cho, E. S.; Heo, T. W.; Prendergast, D.; Urban, J. J.; Wood, B. C.; Allendorf, M. D.; Stavila, V. Nanostructured Metal Hydrides for Hydrogen Storage. *Chem. Rev.* **2018**, *118*, 10775−10839.

(5) Gong, C.; Leite, M. S. Noble Metal Alloys for Plasmonics. *ACS Photonics* **2016**, *3*, 507−513.

(6) Gong, C.; Dias, M. R. S.; Wessler, G. C.; Taillon, J. A.; Salamanca-Riba, L. G.; Leite, M. S. Near-Field Optical Properties of Fully Alloyed Noble Metal Nanoparticles. *Adv. Opt. Mater.* **2017**, *5*, 1600568.

(7) Gong, C.; Kaplan, A.; Benson, Z. A.; Baker, D. R.; McClure, J. P.; Rocha, A. R.; Leite, M. S. Band Structure Engineering by Alloying for Photonics. *Adv. Opt. Mater.* **2018**, *6*, 1800218.

(8) Benson, Z. A.; Gong, C.; Leite, M. S. Optical Response of Nanostructures: From Pure to Alloyed Metals. In *Metal Nanostructures for Photonics*; Kassab, L. R. P., de Araujo, C. B., Eds.; Elsevier, 2019; pp 87−103.

(9) McClure, J. P.; Boltersdorf, J.; Baker, D. R.; Farinha, T. G.; Dzuricky, N.; Villegas, C. P.; Rocha, A. A.; Leite, M. S. Structure−Property-Performance Relationship of Ultrathin Pd−Au Alloy Catalyst Layers for Low-Temperature Ethanol Oxidation in Alkaline Media. *ACS Appl. Mater. Interfaces* **2019**, DOI: 10.1021/acsami.9b01389.

(10) Haffner, C.; Chelladurai, D.; Fedoryshyn, Y.; Josten, A.; Baeuerle, B.; Heni, W.; Watanabe, T.; Cui, T.; Cheng, B.; Saha, S.; Elder, D. L.; Dalton, L. R.; Boltasseva, A.; Shalaev, V. M.; Kinsey, N.; Leuthold, J. Low-Loss Plasmon-Assisted Electro-Optic Modulator. *Nature* **2018**, *556*, 483−486.

(11) Deng, X.; Li, L.; Enomoto, M.; Kawano, Y. Continuously Frequency-Tuneable Plasmonic Structures for Terahertz Bio-Sensing and Spectroscopy. *Sci. Rep.* **2019**, *9*, 3498.

(12) Shao, L.; Zhuo, X.; Wang, J. Advanced Plasmonic Materials for Dynamic Color Display. *Adv. Mater.* **2018**, *30*, 1704338.

(13) West, P. R.; Ishii, S.; Naik, G. V.; Emani, N. K.; Shalaev, V. M.; Boltasseva, A. Searching for Better Plasmonic Materials. *Laser Photonics Rev.* **2010**, *4*, 795−808.

(14) Zhou, L.; Tan, Y.; Wang, J.; Xu, W.; Yuan, Y.; Cai, W.; Zhu, S.; Zhu, J. 3D Self-Assembly of Aluminium Nanoparticles for Plasmon-Enhanced Solar Desalination. *Nat. Photonics* **2016**, *10*, 393.

(15) Maier, S. A.; Brongersma, M. L.; Kik, P. G.; Meltzer, S.; Requicha, A. A. G.; Atwater, H. A. Plasmonics—A Route to Nanoscale Optical Devices. *Adv. Mater.* **2001**, *13*, 1501−1505.

(16) Graells, S.; Alcubilla, R.; Badenes, G.; Quidant, R. Growth of Plasmonic Gold Nanostructures by Electron Beam Induced Deposition. *Appl. Phys. Lett.* **2007**, *91*, 121112.

(17) Thyagarajan, K.; Santschi, C.; Langlet, P.; Martin, O. J. F. Highly Improved Fabrication of Ag and Al Nanostructures for UV and Nonlinear Plasmonics. *Adv. Opt. Mater.* **2016**, *4*, 871−876.

(18) Parashar, P. K.; Komarala, V. K. Engineered Optical Properties of Silver-Aluminum Alloy Nanoparticles Embedded in SiON Matrix for Maximizing Light Confinement in Plasmonic Silicon Solar Cells. *Sci. Rep.* **2017**, *7*, 12520.

(19) Gao, J.; Wang, X.; Yang, B.; Tu, C.; Liang, L.; Zhang, H.; Zhuge, F.; Cao, H.; Zou, Y.; Yu, K.; Xia, F.; Han, Y. Plasmonic AgAl Bimetallic Alloy Nanoparticle/Al2O3 Nanocermet Thin Films with Robust Thermal Stability for Solar Thermal Applications. *Adv. Mater. Interfaces* **2016**, *3*, 1600248.

(20) Hashimoto, Y.; Seniutinas, G.; Balčytis, A.; Juodkazis, S.; Nishijima, Y. Au-Ag-Cu Nano-Alloys: Tailoring of Permittivity. *Sci. Rep.* **2016**, *6*, 25010.

(21) Link, S.; Wang, Z. L.; El-Sayed, M. A. Alloy Formation of Gold−Silver Nanoparticles and the Dependence of the Plasmon Absorption on Their Composition. *J. Phys. Chem. B* **1999**, *103*, 3529−3533.

(22) Kusada, K.; Yamauchi, M.; Kobayashi, H.; Kitagawa, H.; Kubota, Y. Hydrogen-Storage Properties of Solid-Solution Alloys of Immiscible Neighboring Elements with Pd. *J. Am. Chem. Soc.* **2010**, *132*, 15896−15898.

(23) Kakavelakis, G.; Stratakis, E.; Kymakis, E. Synergetic Plasmonic Effect of Al and Au Nanoparticles for Efficiency Enhancement of Air Processed Organic Photovoltaic Devices. *Chem. Commun.* **2014**, *50*, 5285−5287.

(24) Valenti, M.; Venugopal, A.; Tordera, D.; Jonsson, M. P.; Biskos, G.; Schmidt-Ott, A.; Smith, W. A. Hot Carrier Generation and Extraction of Plasmonic Alloy Nanoparticles. *ACS Photonics* **2017**, *4*, 1146−1152.

(25) Green, M. A.; Pillai, S. Harnessing Plasmonics for Solar Cells. *Nat. Photonics* **2012**, *6*, 130.

(26) Parashar, P. K.; Sharma, R. P.; Komarala, V. K. Plasmonic Silicon Solar Cell Comprised of Aluminum Nanoparticles: Effect of Nanoparticles' Self-Limiting Native Oxide Shell on Optical and Electrical Properties. *J. Appl. Phys.* **2016**, *120*, 143104.

(27) Gong, T.; Munday, J. N. Angle-Independent Hot Carrier Generation and Collection Using Transparent Conducting Oxides. *Nano Lett.* **2015**, *15*, 147−152.

(28) Zaleska-Medynska, A.; Marchelek, M.; Diak, M.; Grabowska, E. Noble Metal-Based Bimetallic Nanoparticles: The Effect of the Structure on the Optical, Catalytic and Photocatalytic Properties. *Adv. Colloid Interface Sci.* **2016**, *229*, 80−107.

(29) Zhou, L.; Swearer, D. F.; Zhang, C.; Robatjazi, H.; Zhao, H.; Henderson, L.; Dong, L.; Christopher, P.; Carter, E. A.; Nordlander, P.; Halas, N. J. Quantifying Hot Carrier and Thermal Contributions in Plasmonic Photocatalysis. *Science* **2018**, *362*, 69.

(30) Zhang, C.; Zhao, H.; Zhou, L.; Schlather, A. E.; Dong, L.; McClain, M. J.; Swearer, D. F.; Nordlander, P.; Halas, N. J. Al−Pd Nanodisk Heterodimers as Antenna−Reactor Photocatalysts. *Nano Lett.* **2016**, *16*, 6677−6682.

(31) Wei, S.-H.; Mbaye, A. A.; Ferreira, L. G.; Zunger, A. First-Principles Calculations of the Phase Diagrams of Noble Metals: Cu-Au, Cu-Ag, and Ag-Au. *Phys. Rev. B: Condens. Matter Mater. Phys.* **1987**, *36*, 4163−4185.

(32) Dettelbach, K. E.; He, J.; Johnson, N. J. J.; Huang, A.; Bottomley, A.; Lam, B.; Salvatore, D. A.; Berlinguette, C. P. Kinetic Phases of Ag−Cu Alloy Films Are Accessible through Photodeposition. *J. Mater. Chem. A* **2019**, *7*, 711−715.

(33) Song, J.; Li, H.; Li, J.; Wang, S.; Zhou, S. Fabrication and Optical Properties of Metastable Cu−Ag Alloys. *Appl. Opt.* **2002**, *41*, 5413−5416.

(34) Blaber, M. G.; Arnold, M. D.; Ford, M. J. A Review of the Optical Properties of Alloys and Intermetallics for Plasmonics. *J. Phys.: Condens. Matter* **2010**, *22*, 143201.

(35) Kitamura, R.; Pilon, L.; Jonasz, M. Optical Constants of Silica Glass from Extreme Ultraviolet to Far Infrared at near Room Temperature. *Appl. Opt.* **2007**, *46*, 8118−8133.

(36) Rioux, D.; Vallières, S.; Besner, S.; Muñoz, P.; Mazur, E.; Meunier, M. An Analytic Model for the Dielectric Function of Au, Ag, and Their Alloys. *Adv. Opt. Mater.* **2014**, *2*, 176−182.

(37) Rivory, J. Comparative Study of the Electronic Structure of Noble-Metal-Noble-Metal Alloys by Optical Spectroscopy. *Phys. Rev. B* **1977**, *15*, 3119−3135.

(38) Takenaka, M.; Hashimoto, Y.; Iwasa, T.; Taketsugu, T.; Seniutinas, G.; Balčytis, A.; Juodkazis, S.; Nishijima, Y. First Principles Calculations Toward Understanding SERS of 2,2′-Bipyridyl Adsorbed on Au, Ag, and Au−Ag Nanoalloy. *J. Comput. Chem.* **2019**, *40*, 925−932.

(39) Nishijima, Y.; Shimizu, S.; Kurihara, K.; Hashimoto, Y.; Takahashi, H.; Balčytis, A.; Seniutinas, G.; Okazaki, S.; Juodkazytė, J.; Iwasa, T.; Taketsugu, T.; Tominaga, Y.; Juodkazis, S. Optical Readout of Hydrogen Storage in Films of Au and Pd. *Opt. Express* **2017**, *25*, 24081−24092.

(40) Chen, K.; Dao, T. D.; Ishii, S.; Aono, M.; Nagao, T. Infrared Aluminum Metamaterial Perfect Absorbers for Plasmon-Enhanced Infrared Spectroscopy. *Adv. Funct. Mater.* **2015**, *25*, 6637−6643.

(41) Hylton, N. P.; Li, X. F.; Giannini, V.; Lee, K.-H.; Ekins-Daukes, N. J.; Loo, J.; Vercruysse, D.; Van Dorpe, P.; Sodabanlu, H.; Sugiyama, M.; Maier, S. A. Loss Mitigation in Plasmonic Solar Cells: Aluminium Nanoparticles for Broadband Photocurrent Enhancements in GaAs Photodiodes. *Sci. Rep.* **2013**, *3*, 2874.

(42) Whiteoak, C. J.; Kielland, N.; Laserna, V.; Escudero-Adán, E. C.; Martin, E.; Kleij, A. W. A Powerful Aluminum Catalyst for the Synthesis of Highly Functional Organic Carbonates. *J. Am. Chem. Soc.* **2013**, *135*, 1228−1231.

(43) Farinha, T. G.; Gong, C.; Benson, Z. A.; Leite, M. S. Magnesium for Transient Photonics. *ACS Photonics* **2019**, *6*, 272−278.

(44) Vignolini, S.; Yufa, N. A.; Cunha, P. S.; Guldin, S.; Rushkin, I.; Stefik, M.; Hur, K.; Wiesner, U.; Baumberg, J. J.; Steiner, U. A 3D Optical Metamaterial Made by Self-Assembly. *Adv. Mater.* **2012**, *24*, OP23−OP27.

(45) Duan, X.; Kamin, S.; Liu, N. Dynamic Plasmonic Colour Display. *Nat. Commun.* **2017**, *8*, 14606.

(46) Rodríguez-González, B.; Burrows, A.; Watanabe, M.; Kiely, C. J.; Liz Marzán, L. M. Multishell Bimetallic AuAg Nanoparticles: Synthesis, Structure and Optical Properties. *J. Mater. Chem.* **2005**, *15*, 1755−1759.

(47) Rioux, D.; Meunier, M. Seeded Growth Synthesis of Composition and Size-Controlled Gold−Silver Alloy Nanoparticles. *J. Phys. Chem. C* **2015**, *119*, 13160−13168.

(48) Guerin, S.; Hayden, B. E.; Lee, C. E.; Mormiche, C.; Russell, A. E. High-Throughput Synthesis and Screening of Ternary Metal Alloys for Electrocatalysis. *J. Phys. Chem. B* **2006**, *110*, 14355−14362.

(49) Ma, M.; Hansen, H. A.; Valenti, M.; Wang, Z.; Cao, A.; Dong, M.; Smith, W. A. Electrochemical Reduction of CO2 on Compositionally Variant Au-Pt Bimetallic Thin Films. *Nano Energy* **2017**, *42*, 51−57.

(50) Yi, L.; You-ping, C.; Han, S.; Gang, Z. Hydrogen Gas Sensor Based on Palladium and Yttrium Alloy Ultrathin Film. *Rev. Sci. Instrum.* **2012**, *83*, 125003.

(51) Chen, P.-C.; Liu, G.; Zhou, Y.; Brown, K. A.; Chernyak, N.; Hedrick, J. L.; He, S.; Xie, Z.; Lin, Q.-Y.; Dravid, V. P.; O'Neill-Slawecki, S. A.; Mirkin, C. A. Tip-Directed Synthesis of Multimetallic Nanoparticles. *J. Am. Chem. Soc.* **2015**, *137*, 9167−9173.

(52) Nugroho, F. A. A.; Iandolo, B.; Wagner, J. B.; Langhammer, C. Bottom-Up Nanofabrication of Supported Noble Metal Alloy Nanoparticle Arrays for Plasmonics. *ACS Nano* **2016**, *10*, 2871−2879.

(53) Verma, S.; Rao, B. T.; Detty, A. P.; Ganesan, V.; Phase, D. M.; Rai, S. K.; Bose, A.; Joshi, S. C.; Kukreja, L. M. Surface Plasmon Resonances of Ag-Au Alloy Nanoparticle Films Grown by Sequential Pulsed Laser Deposition at Different Compositions and Temperatures. *J. Appl. Phys.* **2015**, *117*, 133105.

(54) Svedberg, F.; Li, Z.; Xu, H.; Käll, M. Creating Hot Nanoparticle Pairs for Surface-Enhanced Raman Spectroscopy through Optical Manipulation. *Nano Lett.* **2006**, *6*, 2639−2641.

(55) Kravets, V. G.; Kabashin, A. V.; Barnes, W. L.; Grigorenko, A. N. Plasmonic Surface Lattice Resonances: A Review of Properties and Applications. *Chem. Rev.* **2018**, *118*, 5912−5951.

(56) Rechberger, W.; Hohenau, A.; Leitner, A.; Krenn, J. R.; Lamprecht, B.; Aussenegg, F. R. Optical Properties of Two Interacting Gold Nanoparticles. *Opt. Commun.* **2003**, *220*, 137−141.

(57) Kadkhodazadeh, S.; Nugroho, F. A. A.; Langhammer, C.; Beleggia, M.; Wagner, J. B. Optical Property−Composition Correlation in Noble Metal Alloy Nanoparticles Studied with EELS. *ACS Photonics* **2019**, *6*, 779−786.

(58) Francis, L. D.; Rivas, J.; José-Yacamán, M. Understanding the Structure of Nanocatalysts with High Resolution Scanning/Transmission Electron Microscopy. *IOP Conf. Ser.: Mater. Sci. Eng.* **2014**, *55*, 012005.

(59) Chen, P.-C.; Liu, X.; Hedrick, J. L.; Xie, Z.; Wang, S.; Lin, Q.-Y.; Hersam, M. C.; Dravid, V. P.; Mirkin, C. A. Polyelemental Nanoparticle Libraries. *Science* **2016**, *352*, 1565.

DOI: 10.1021/acs.accounts.9b00153
Acc. Chem. Res. 2019, 52, 2881−2891